Vol. 126: 167–172, 2017
https://doi.org/10.3354/dao03166

DISEASES OF AQUATIC ORGANISMS
Dis Aquat Org

Published October 18

NOTE

Locally extensive meningoencephalitis caused by *Miamiensis avidus* (syn. *Philasterides dicentrarchi*) in a zebra shark

Wen-Ta Li[1], Chieh Lo[2], Chen-Yi Su[2], Hsuan Kuo[1], Susanne Je-Han Lin[1], Hui-Wei Chang[1], Victor Fei Pang[1], Chian-Ren Jeng[1,*]

[1]Graduate Institute of Molecular and Comparative Pathobiology, School of Veterinary Medicine, National Taiwan University, No. 1, Sec. 4, Roosevelt Rd, Taipei 10617, Taiwan, ROC

[2]Farglory Ocean Park, No.189, Yenliao Village, Shoufong Township, Hualien, Taiwan, ROC

ABSTRACT: Scuticociliatosis, caused by ciliated protozoa in the subclass Scuticociliatia of the phylum Ciliophora, can cause fatal disease in teleost fish species. However, information on scuticociliatosis in elasmobranchs is still scarce. In this report, we describe a case of locally extensive meningoencephalitis caused by *Miamiensis avidus* (syn. *Philasterides dicentrarchi*) in a 2 yr old captive zebra shark *Stegostoma fasciatum*. Granulocytic meningoencephalitis was observed through histological assessment. Inflammation was confined to the ventral aspect of the brain with a large number of ciliated protozoa, transforming into non-suppurative meningitis in the lateral aspect, and gradually vanished in the dorsal aspect. No histopathological and polymerase chain reaction (PCR) evidence of systemic dissemination of *M. avidus* was found. PCR targeting the gene coding the small-subunit ribosomal RNA (*SSUrRNA*) of *M. avidus* was performed on the brain, liver, and gill tissues, and only brain tissue yielded a positive result. The DNA sequences from amplicons of the protozoal *SSUrRNA* gene were completely matched to that of *M. avidus*. The distribution of protozoa in the current case was mainly located in the brain and suggests the possibility of a direct neural invasive pathway of *M. avidus* through the nasal cavity/ampullary system and/or a unique tissue tropism of *M. avidus* specific to the brain in zebra sharks. Further investigations on the pathogenesis of *M. avidus* in elasmobranchs, especially zebra sharks, are needed.

KEY WORDS: Scuticociliatosis · Scuticociliatosis · Tissue tropism · Neural invasive pathway · Small-subunit ribosomal RNA (*SSUrRNA*) · Ciliated protozoa

INTRODUCTION

Scuticociliatosis is caused by histophagous ciliated protozoa in the subclass Scuticociliatia of the phylum Ciliophora. Infection with the scuticociliate *Miamiensis avidus* (syn. *Philasterides dicentrarchi*) in teleost fish species can occur by invasion through compromised skin and/or gills with subsequent spread to other internal organs via blood circulation, resulting in necrotizing inflammation and thereby causing fatal disease in the hosts (Iglesias et al. 2001, Puig et al. 2007, Jin et al. 2009, Moustafa et al. 2010a, Kubiski et al. 2011, Harikrishnan et al. 2012, Di Cicco et al. 2013). Only 3 publications have reported on scuticociliatosis in elasmobranchs, and thus information on scuticociliatosis in sharks is still scarce (Goertz 2004, Garner 2013, Stidworthy et al. 2014). Here we describe a case of locally extensive menin-

*Corresponding author: crjeng@ntu.edu.tw

goencephalitis with abundant intralesional *M. avidus* in a captive zebra shark *Stegostoma fasciatum*. Our findings suggest the possibility of a direct neural invasive pathway of *M. avidus* through the nasal cavity/ampullary system and/or a unique tissue tropism of *M. avidus* specific to brain in zebra sharks.

MATERIALS AND METHODS

A 16.5 kg, wild-caught, 2 yr old female zebra shark had been kept in an indoor seawater pool for approximately 2 yr with many other species of teleosts and elasmobranchs. The natural seawater was drawn, treated in a sedimentation basin with germicidal ultraviolet light, and then added into the indoor seawater pool. The seawater in the pool was routinely treated through a closed filtration system with a sedimentation basin, germicidal ultraviolet light, protein skimming, biological filtering, and ozone disinfection. During the 2 yr interval, the mean ± standard deviation (SD) of water temperature was 25.3 ± 0.4°C, salinity was 33.4 ± 0.8 ppt, pH was 7.6 ± 0.2, and the dissolved oxygen level was 6.7 ± 0.2 ppm. The zebra shark showed poor appetite and lethargy on 17 November 2016. The next day, the animal was floating upside down and biting its own tail. Hematology and plasma biochemistry revealed increased albumin (1.5 g dl^{-1}) and increased creatine kinase (5259 U l^{-1}). The reference ranges of hematology and plasma biochemistry were based on previous studies in other shark species (Haman et al. 2012, Alexander et al. 2016). In addition, no remarkable findings were noted on blood smears. Dexamethasone (0.1 mg kg^{-1}, IM) and ceftazidime (22 mg kg^{-1}, IM) were given, but the animal was found dead on the morning of 19 November 2016. In this pool, no new animals had been introduced recently, and no other animals were affected or had died in the meantime.

A complete necropsy with standardized procedures was performed, and representative tissue samples, including the brain, gills, heart, gastrointestinal tract, liver, pancreas, spleen, kidneys, and gonads, were collected, fixed in 10% neutral buffered formalin, processed routinely, sectioned at 4 µm, and stained with hematoxylin and eosin (H&E). Polymerase chain reaction (PCR) with subsequent DNA sequencing using formalin-fixed, paraffin-embedded (FFPE) tissues from brain, liver, and gills was performed separately to identify the species of ciliated protozoa. DNA was extracted from 80 µm sections of tissue using the QIAamp DNA FFPE Tissue Kit (Qiagen) and used as PCR templates. Primer sets targeting the gene coding the small-subunit ribosomal RNA (*SSUrRNA*) of scutiociliate (PSSU1: 5′-GAG AAA CGG CTA CCA CAT CTA-3′ and PSSU2: 5′-CAA GGT AAA GAG CCT ACT CCA-3′) were used with an expected product size of 350 bp (Rossteuscher et al. 2008, Di Cicco et al. 2013). To validate the quality of the extracted DNA, a primer set (forward: 5′-CTG GTT GAT CCT GCC AG-3′; reverse: 5′-ACC AGA CTT GCC CTC C-3′) targeting the rRNA gene was used in a PCR with an expected product size of 560 bp (Díez et al. 2001). The cycling conditions included an initial denaturation of 5 min at 94°C followed by 35 cycles of denaturation for 30 s at 94°C, annealing for 1 min at different temperatures (60°C for primer sets targeting the eukaryotic rRNA gene and 55°C for primer sets targeting the *SSUrRNA* gene), and an extension for 2 min at 72°C, with a final extension of 5 min at 72°C. The PCR reactions were carried out with commercial reagents (OnePCR, GeneDireX). The obtained amplicons were directly sequenced and compared with sequences available in GenBank using the Basic Local Alignment Search Tool (BLAST) server from the National Center for Biotechnology Information.

RESULTS

Gross examination revealed that the ventral side of the body had multifocal erythema. Upon opening the body cavity, multifocal ecchymoses of varying size were found on the liver surface (Fig. 1A). The brain showed multifocal accumulations of white cloudy fragile material (Fig. 1B). Microscopically, the meninges at the ventral and lateral aspect of the brain were diffusely thickened with increased cellularity, and the underlying brain parenchyma showed multifocal to coalescing foci of neuropil rarefaction and liquefaction (Fig. 2A,B). In the ventral aspect of the brain, abundant granulocytes with scattered mononuclear inflammatory cells infiltrated the meninges and extended into the underlying brain parenchyma with multifocal perivascular cuffing. Also found in affected areas were numerous round to oval ciliated protozoa of approximately 20–25 µm in diameter, which had a hyperchromatic round to oval macronucleus (approximately 10 µm in diameter) and a variably sized, pale basophilic vesicular cytoplasm containing varying numbers of homogeneous eosinophilic intracytoplasmic globules (Fig. 2C). The granulocytic meningoencephalitis was confined to the ventral aspect of the brain, transforming into non-suppurative meningitis in the lateral aspect (Fig. 2D), and gradu-

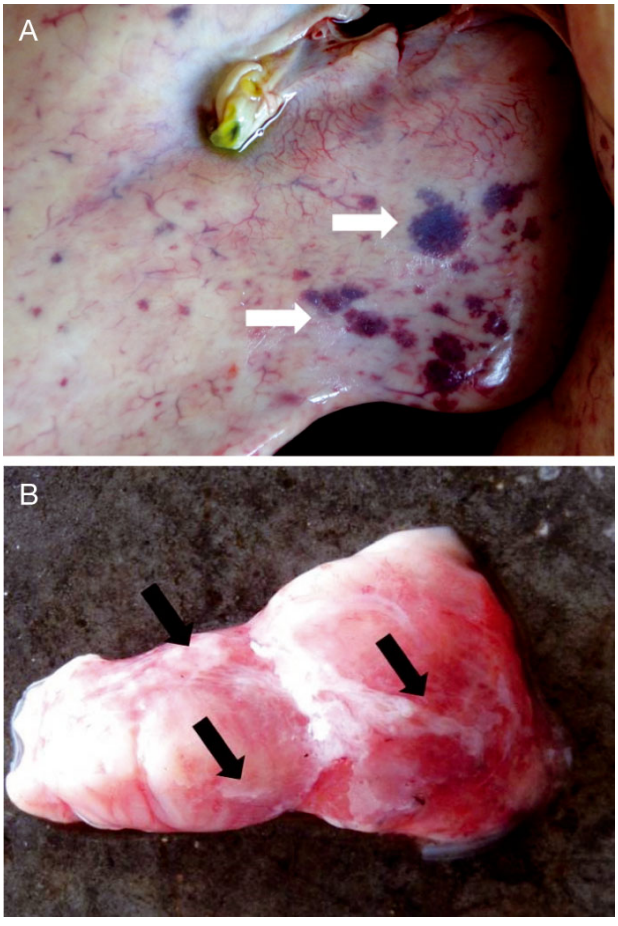

Fig. 1. Gross findings of the liver and brain of a zebra shark *Stegostoma fasciatum*. (A) Ecchymotic hemorrhages of 0.1 to 0.5 cm in diameter on the liver surface (white arrows). (B) White cloudy fragile material can be seen on the surfaces of the cerebrum and cerebellum (black arrows)

ally vanished in the dorsal aspect. The normal architecture of the liver was multifocally disrupted by the necrohemorrhagic areas infiltrated by low to moderate numbers of granulocytes (Fig. 2E), but ciliated protozoa were not observed. Furthermore, no evidence of systemic scuticociliatosis, such as the presence of ciliated protozoa, vasculitis, and intravascular ciliated protozoa, was found in any other organ evaluated.

Only the brain tissue was positive for the PCR targeting the *SSUrRNA* gene (Fig. 3), and the DNA sequences from amplified amplicons of the *SSUrRNA* gene were completely matched to that of *Miamiensis avidus* (100% identity with GenBank accession KX259260 and others). The results of histopathology, PCR, and DNA sequencing confirmed the final diagnosis of locally extensive meningoencephalitis caused by *M. avidus*.

DISCUSSION

In previous publications, ciliate infections in sharks have been identified in skin, gills, kidneys, pancreas, oviduct, claspers, brain, and liver (Goertz 2004, Garner 2013, Stidworthy et al. 2014). One case report covering an acutely lethal scuticociliate infection in zebra sharks, Port Jackson sharks *Heterodontus portusjacksoni*, and Japanese horn sharks *H. japonicus* found that necrotizing hepatitis, necrotizing meningoencephalitis, and thrombosing branchitis with necrotizing vasculitis and/or intravascular fibrinocellular thrombi were characteristic lesions for systemic scuticociliatosis (Stidworthy et al. 2014). In addition, *Miamiensis avidus* was found in the brains of affected zebra sharks (3/4), but not in the brains of Port Jackson sharks (0/3) or a Japanese horn shark (0/1) (Stidworthy et al. 2014). Therefore, we speculate that there might be a different infective pathway of *M. avidus* for zebra sharks. A previous study of experimental infection in Japanese flounders indicated that *M. avidus* were frequently observed in the optic and/or olfactory nerve and found in peripheral nerve fibers of affected teleost fishes (Moustafa et al. 2010b). Moustafa et al. (2010b) also found that the lesions in the brain were more severe than those in the gills and skin, suggesting the possibility of a neural invasive pathway through periorbital and nasal routes with subsequent intravascular and/or intraneural dissemination (Moustafa et al. 2010b). Furthermore, neural invasive pathogens have been recognized in sharks. For example, a previous case report found ampullary system infection and septicemia caused by *Serratia marcescens* in a bonnethead shark *Sphyrna tiburo* (Camus et al. 2013), providing evidence that this may be a viable route of entry for *M. avidus*.

In the present case, the tissue distribution of *M. avidus* was confined to the brain and confirmed by histopathological and molecular investigations. Therefore, we speculate that *M. avidus* might have directly invaded the central nervous system via the nasal cavity/ampullary system rather than via blood circulation. However, Garner (2013) stated that protozoa could be difficult to find in tissue sections. Although PCR tests were negative in liver and gills, the possibility of extremely low numbers of *M. avidus* in the blood circulation cannot be completely ruled out. Therefore, it is also suspected that (1) infection of *M. avidus* might be established in the brain and then disseminated systemically, and/or (2) *M. avidus* might have tissue tropism specific to the brain in the zebra shark.

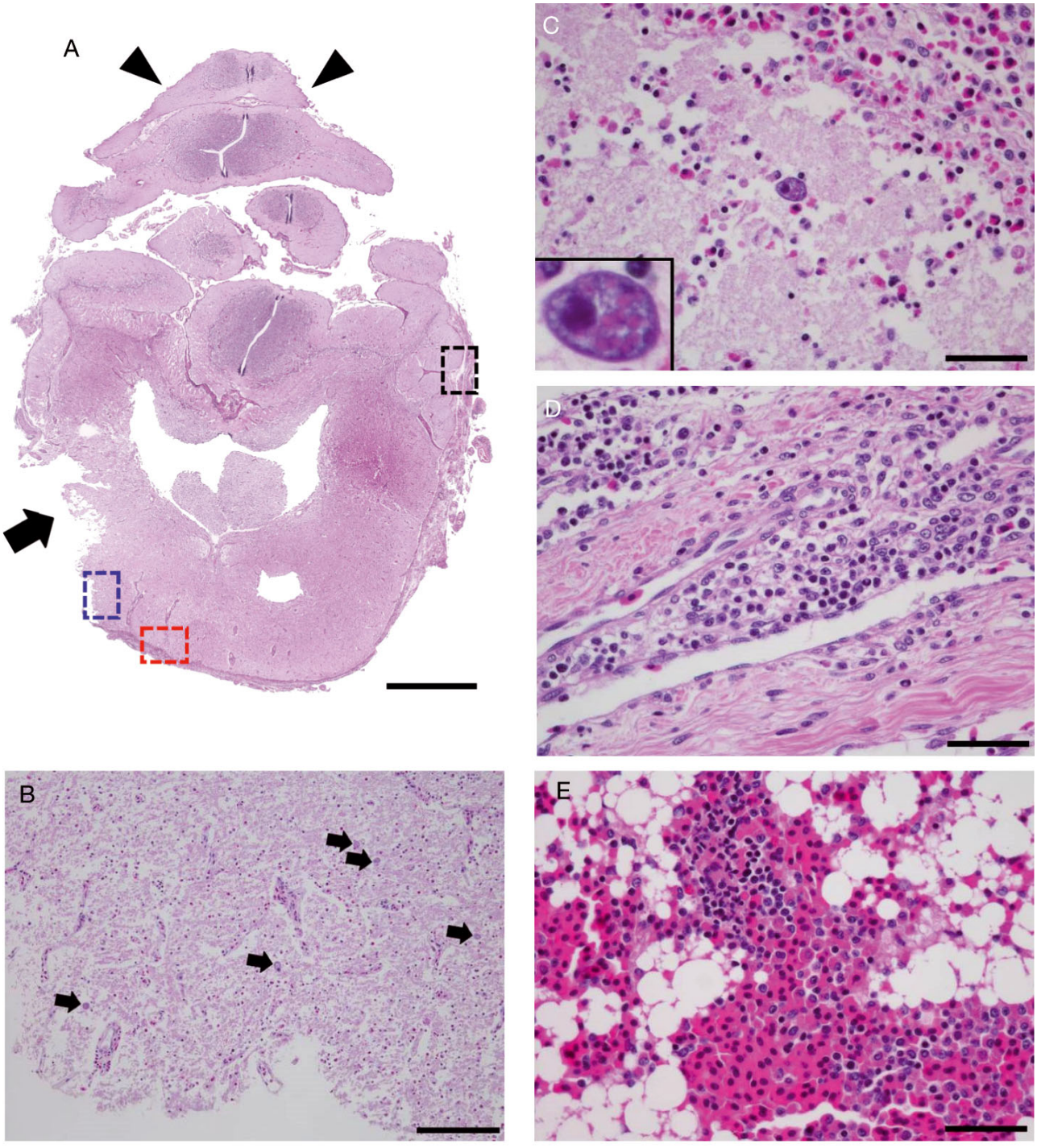

Fig. 2. Histopathological findings (H&E stain) of meningoencephalitis and hepatitis in a zebra shark *Stegostoma fasciatum*. (A) Meninges are extensively thickened locally in the ventral and lateral aspects and gradually diminish in the dorsal aspect (arrowheads). A focal area with severe tissue loss is noted at the lateral-ventral side of brain (black arrow). Scale bar = 2 mm. (B) Lesions found around the area of brain tissue loss (blue dashed rectangle in panel A). The neuropil is rarefied due to diffuse edema and liquefactive necrosis with scattered ciliated protozoa (black arrows). Scale bar = 100 µm. (C) Lesions in the ventral aspect of the brain (red dashed rectangle in panel A). Abundant granulocytes infiltrate the meninges and extend into the underlying parenchyma with scattered ciliated protozoa. Scale bar = 100 µm. Inset: The protozoan organism is covered by rows of cilia, contains a hyperchromatic round to oval macronucleus, and has vesicular basophilic cytoplasm with several homogeneous eosinophilic intracytoplasmic droplets. (D) Lesion in the lateral aspect of the brain (black dashed rectangle in panel A). Mononuclear inflammatory cells (macrophages and lymphocytes predominant with scattered granulocytes) infiltrate the perivascular regions of the meninges. Scale bar = 50 µm. (E) Normal architecture of the liver was multifocally disrupted by the necrohemorrhagic lesions, which are composed of hemorrhages and necrotic cell debris with granulocyte infiltration. Scale bar = 50 µm

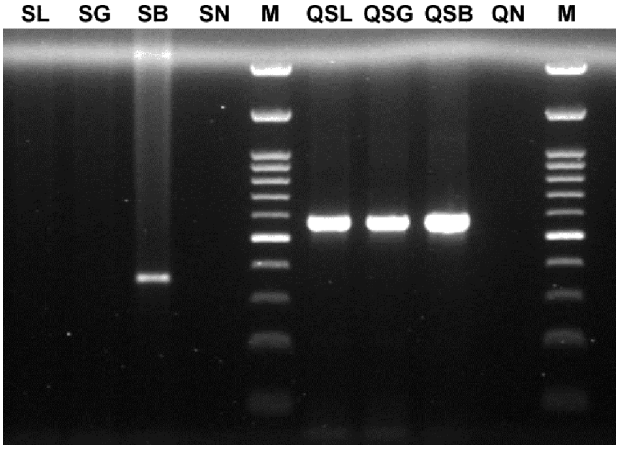

Fig. 3. Agarose gel electrophoresis (1.5%) of polymerase chain reaction products. Samples: DNA extracted from the liver (SL), gills (SG), and brain (SB) tissues of a zebra shark *Stegostoma fasciatum* with a primer set targeting small-subunit ribosomal RNA (*SSUrRNA*) gene of *Miamiensis avidus*. SN: negative control (deuterium-depleted water) with a primer set targeting *SSUrRNA* of *M. avidus*. Quality controls: DNA extracted from the liver (QSL), gills (QSG), and brain (QSB) tissues with primers targeting the eukaryotic rRNA gene; QN: negative control (deuterium-depleted water) with primers targeting the eukaryotic rRNA gene. M: 100 bp ladder marker (Star-100bp DNA Ladder, OneStar)

The role of the relatively low pH of the seawater in the affected zebra shark's enclosure is unknown but was considered as a potential contributing factor. Generally, the pH value of seawater should be between 7.8 and 8.4, and it is best kept between 8.1 and 8.3 (Noga 2010). The negative effects of environmental acidification in sharks are still largely unknown, but decreased pH has been shown to compromise the immune function in carp *Cyprinus carpio* (Nagae et al. 2001). Long-term environmental acidification may have caused immune compromise in the affected zebra shark and/or may have supported conditions promoting *M. avidus* growth and infection. An *in vitro* study demonstrated that the optimal pH value for the growth of *M. avidus* was 7.2 (Iglesias et al. 2003). To our knowledge, only 1 study on the outbreak of *M. avidus* in marine fish (Australian potbellied seahorses *Hippocampus abdominalis*) mentioned the pH value (7.5), and that value was similar to the one in our case.

Our findings are suggestive of either a direct neural invasive pathway of *M. avidus* through the nasal cavity and/or the ampullary system or a unique tissue tropism of *M. avidus* specific to brain in zebra sharks. The role of decreased pH of seawater in this case is unknown but could potentially play a role in immunocompromising the host and in the pathogenicity of the pathogen. To understand the pathogenesis of this emerging pathogen, further investigations into the marine environment, *M. avidus*, and elasmobranchs, especially zebra sharks, are warranted.

Acknowledgements. We thank all the personnel of Farglory Ocean Park for sample collection and storage, and the pathology residents (Dr. Phoebe Chi-Fei Kao) and professors (Dr. Fun-In Wang and Dr. Chen-Hsuan Liu) of the Graduate Institute of Molecular and Comparative Pathobiology, National Taiwan University, for idea discussion.

LITERATURE CITED

Alexander AB, Parkinson LA, Grant KR, Carlson E, Campbell TW (2016) The hemic response of white-spotted bamboo sharks (*Chiloscyllium plagiosum*) with inflammatory disease. Zoo Biol 35:251–259

Camus A, Berliner A, Clauss T, Hatcher N, Marancik D (2013) *Serratia marcescens* associated ampullary system infection and septicaemia in a bonnethead shark, *Sphyrna tiburo* (L.). J Fish Dis 36:891–895

Di Cicco E, Paradis E, Stephen C, Turba ME, Rossi G (2013) Scuticociliatid ciliate outbreak in Australian potbellied seahorse, *Hippocampus abdominalis* (Lesson, 1827): clinical signs, histopathologic findings, and treatment with metronidazole. J Zoo Wildl Med 44:435–440

Díez B, Pedrós-Alió C, Marsh TL, Massana R (2001) Application of denaturing gradient gel electrophoresis (DGGE) to study the diversity of marine picoeukaryotic assemblages and comparison of DGGE with other molecular techniques. Appl Environ Microbiol 67:2942–2951

Garner MM (2013) A retrospective study of disease in elasmobranchs. Vet Pathol 50:377–389

Goertz CEC (2004) Protozoal diseases of elasmobranchs. In: Smith M (ed) The elasmobranch husbandry manual: captive care of sharks, rays, and their relatives. Ohio Biological Survey, Columbus, OH, p 417–426

Haman KH, Norton TM, Thomas AC, Dove AD, Tseng F (2012) Baseline health parameters and species comparisons among free-ranging Atlantic sharpnose (*Rhizoprionodon terraenovae*), bonnethead (*Sphyrna tiburo*), and spiny dogfish (*Squalus acanthias*) sharks in Georgia, Florida, and Washington, USA. J Wildl Dis 48:295–306

Harikrishnan R, Jin CN, Kim JS, Balasundaram C, Heo MS (2012) *Philasterides dicentrarchi*, a histophagous ciliate causing scuticociliatosis in olive flounder, *Philasterides dicentrarchi* [sic]—histopathology investigations. Exp Parasitol 130:239–245

Iglesias R, Paramá A, Alvarez MF, Leiro J, Fernández J, Sanmartín ML (2001) *Philasterides dicentrarchi* (Ciliophora, Scuticociliatida) as the causative agent of scuticociliatosis in farmed turbot *Scophthalmus maximus* in Galicia (NW Spain). Dis Aquat Org 46:47–55

Iglesias R, Parama A, Alvarez MF, Leiro J, Aja C, Sanmartin ML (2003) In vitro growth requirements for the fish pathogen *Philasterides dicentrarchi* (Ciliophora, Scuticociliatida). Vet Parasitol 111:19–30

Jin CN, Harikrishnan R, Moon YG, Kim MC and others (2009) Histopathological changes of Korea cultured olive flounder, *Paralichthys olivaceus* due to scuticociliatosis

caused by histophagous scuticociliate, *Philasterides dicentrarachi*. Vet Parasitol 161:292–301

Kubiski SV, Howerth EW, Clauss TM, Berliner AL, Camus AC (2011) Pathology in practice. Scuticociliatosis. J Am Vet Med Assoc 238:301–303

Moustafa EM, Naota M, Morita T, Tange N, Shimada A (2010a) Pathological study on the scuticociliatosis affecting farmed Japanese flounder (*Paralichthys olivaceus*) in Japan. J Vet Med Sci 72:1359–1362

Moustafa EM, Tange N, Shimada A, Morita T (2010b) Experimental scuticociliatosis in Japanese flounder (*Paralichthys olivaceus*) infected with *Miamiensis avidus*: pathological study on the possible neural routes of invasion and dissemination of the scuticociliate inside the fish body. J Vet Med Sci 72:1557–1563

Nagae M, Ogawa K, Kawahara A, Yamaguchi M, Nishimura T, Ito F (2001) Effect of acidification stress on endocrine and immune functions in carp, *Cyprinus carpio.* Water Air Soil Pollut 130:893–898

Noga EJ (2010) Fish disease: diagnosis and treatment. Wiley-Blackwell, Ames, IA

Puig L, Traveset R, Palenzuela O, Padrós F (2007) Histopathology of experimental scuticociliatosis in turbot *Scophthalmus maximus.* Dis Aquat Org 76:131–140

Rossteuscher S, Wenker C, Jermann T, Wahli T, Oldenberg E, Schmidt-Posthaus H (2008) Severe scuticociliate (*Philasterides dicentrarchi*) infection in a population of sea dragons (*Phycodurus eques* and *Phyllopteryx taeniolatus*). Vet Pathol 45:546–550

Stidworthy MF, Garner MM, Bradway DS, Westfall BD and others (2014) Systemic scuticociliatosis (*Philasterides dicentrarchi*) in sharks. Vet Pathol 51:628–632

Editorial responsibility: Dieter Steinhagen, Hannover, Germany

Submitted: June 6, 2017; Accepted: August 9, 2017
Proofs received from author(s): September 28, 2017